Pergamon

Bioorganic & Medicinal Chemistry Letters 11 (2001) 1157–1160

BIOORGANIC & MEDICINAL CHEMISTRY LETTERS

Quinazolines as Cyclin Dependent Kinase Inhibitors

Thais M. Sielecki,[a,*] Tricia L. Johnson,[a] Jie Liu,[a] Jodi K. Muckelbauer,[a] Robert H. Grafstrom,[a] Sarah Cox,[a] John Boylan,[a] Catherine R. Burton,[a] Haiying Chen,[a] Angela Smallwood,[a] Chong-Hwan Chang,[a] Michael Boisclair,[b] Pamela A. Benfield,[a] George L. Trainor[a] and Steven P. Seitz[a]

[a]*The DuPont Pharmaceuticals Company, Wilmington, DE 19880-0500, USA*
[b]*Mitotix Inc., Cambridge, MA 02139, USA*

Received 22 December 2000; accepted 2 March 2001

Abstract—Quinazolines have been identified as inhibitors of CDK4/D1 and CDK2/E. Aspects of the SAR were investigated using solution-phase, parallel synthesis. An X-ray crystal structure was obtained of quinazoline **51** bound in CDK2 and key interactions within the ATP binding pocket are defined.

Interruption of the cell cycle is one approach in the treatment of proliferative diseases. The phases of the cell cycle are driven by cyclin-dependent kinases[1] (CDK), serine- and threonine-specific kinases, which act to modulate levels of protein phosphorylation using adenosine triphosphate (ATP) as a phosphate donor. Several reviews of the biology of the CDK family of kinases have been published.[2]

Several cores have been reported as potent CDK inhibitors including flavones (flavopiridol),[3] azepines (paullones),[4] and purines.[5] Here, we report on the use of quinazolines as CDK inhibitors. Quinazoline **1** is a CDK inhibitor found through screening which shows modest potency for CDK4/D1 ($IC_{50} = 24\,\mu M$), CDK2/E ($IC_{50} = 13.5\,\mu M$) and CDK1/B (also known as CDC2/B) ($IC_{50} = 35\,\mu M$). The compound has modest activity in an HCT 116 cancer cell line ($IC_{50} = 15\,\mu M$) but did not inhibit c-Abl (a tryosine kinase), PKC, or PKA. This quinazoline was determined to be ATP competitive similar to quinazolines found to be inhibitors of tyrosine kinases.[6]

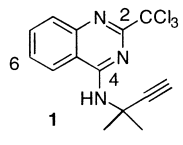

1

In our search for potent and selective CDK inhibitors we explored the impact that R^2, R^4, and R^6 substitution has on the in vitro CDK inhibition of this series. An X-ray crystal structure of **51** revealed key binding elements.

The R^2 substituents were installed using one of three routes. The dichloroquinazoline **2** was reacted with an appropriate amine in the presence of triethyl amine in tetrahydrofuran to give the R^4 substituted chloride **3**, which was then exposed to aniline at 100 °C overnight to yield the R^2 anilino substituted analogues (Scheme 1).

When R^2 is a trichloromethyl moiety it was installed via reaction of aniline **5** with trichloroacetonitrile in HCl saturated dioxane. The resultant chloride was then reacted with an appropriate amine to give the R^4 amino substituted **6** (Scheme 2).

Alternatively, when R^2 is a trifluoromethyl or pentafluoroethyl group, the amide **7** was cyclized to the quinazolinone **8** by reacting with an appropriate ester in

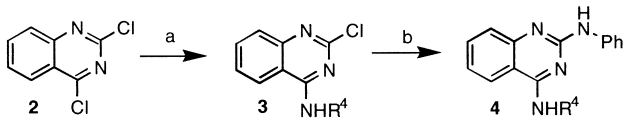

Scheme 1. (a) H_2NR, Et_3N, THF, overnight; (b) H_2NPh, 100–115 °C, overnight.

*Corresponding author. Tel.: +1-302-695-8051; fax: +1-302-695-1502; e-mail: thais.m.sielecki@dupontpharma.com

0960-894X/01/$ - see front matter
PII: S0960-894X(01)00185-8

the presence of NaOEt in ethanol. With the R^2 group installed the quinazolinone was converted to the chloride **9**, which was then reacted with the appropriate amine to give the R^4 amino substituted **10** (Scheme 3).

In evaluating the R^4 position a parallel synthesis approach was employed (Scheme 3). In a solution-phase, parallel synthesis format, chloride **9** ($R^6 = H$) was allowed to react with the appropriate primary or secondary amine in THF at room temperature overnight. The reactions were then quenched with (aminomethyl)polystyrene resin followed by DOWEX-50W-H to remove residual starting materials. Following this protocol, a total of 139 amines were reacted with **9**. This resulted in 124 evaluable compounds with acceptable mass spectral analyses and greater than 85% purity by HPLC analysis. Compounds that had >50% inhibition in the enzyme assays were resynthesized as discretes following the procedures outlined above.

Compounds with substitution at the 6-position were synthesized following Scheme 3, starting with the appropriately substituted aryl moiety. When R^6 was an aryl group, Suzuki chemistry was employed (Scheme 4).

It was shown that small, electron withdrawing, non-ionizable substituents such as trifluoromethyl and trichloromethyl are preferred at R^2 (Table 1). Compound **13** (CDK2/E $IC_{50} = 6.1\,\mu M$) showed approximately 4-fold selectivity for CDK2/E as compared to CDK2/A and CDK1/B and 2-fold selectivity over CDK4/D. The compound was shown to be selective against PKC and PKA. Cell cycle effects were consistent with CDK2/CDK4 inhibition (reversible G1 arrest in fibroblasts). Analogue **14**, the trifluoro version of **13**, showed a similar profile to **13** but with greater potency for CDK2/E ($IC_{50} = 1.53\,\mu M$).

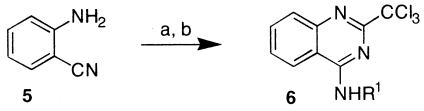

Scheme 2. (a) CCl_3CN, dioxane, HCl (g); (b) H_2NR, Et_3N, THF, overnight.

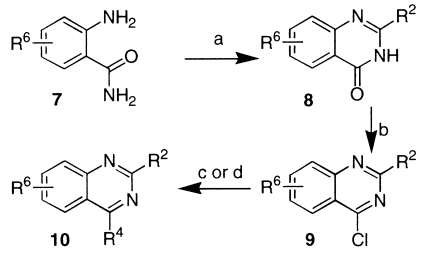

Scheme 3. (a) RCO_2Et, NaOEt, EtOH; (b) $POCl_3$/reflux or $POCl_3$, CH_3CN, *N*,*N*-dimethylaniline; (c) NHR′, THF, rt to reflux; (d) (i) NHR^1R^2, THF, rt overnight; (ii) resin quench with (aminomethyl)-polystyrene followed by DOWEX-50W-H.

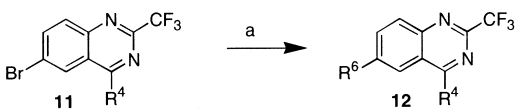

Scheme 4. (a) $RB(OH)_2$, 2 M Na_2CO_3, TBABr, EtOH, $Pd(PPh_3)_4$, toluene, reflux overnight.

With the R^2 SAR defined, we explored the 4-position (Table 2). Branched alkyl groups such as *t*-butyl (**14**) and *t*-amyl (**22**) are preferred. Longer groups such as *n*-butyl (inactive at 50 μM) are inactive as are groups added to increase hydrogen bonding such as sulfonamides (**23**) and 2-methylpentylamine (**24**). Benzyl substitution was modestly effective with electron withdrawing substitution on the benzyl moiety rendering the compounds more potent for CDK2/E (**28**, **29**). Interestingly, the binding pocket distinguishes between the *R* and *S* isomers of the 2-methylbenzylamine **30**. The *R*-isomer **31** has a 10-fold increased potency over the *S*-isomer **32** in the CDK2/E assay. Substitution on the aryl ring of the benzyl group did not improve the potency of this substituent as seen for **33**. The *gem* dimethyl **34** showed activity averaging between **32** and **31**. Overall, the data suggest that there is a size constraint to the binding pocket in the area of the 4-position.

Aromatic ring substitution at the 6-position was also investigated (Table 3). Improved potency was observed

Table 1. Quinazoline substitution at the 2-position ($R^4 = NHt\text{-Bu}$, $R^6 = H$)[a]

Compounds	R^2	CDK4 IC_{50} (μM)	CDK2 IC_{50} (μM)
13[b]	CCl_3	11.9±0.0	6.1±0.0
14	CF_3	14.3±3.4	1.5±0.5
15	CF_2CF_3	>20.0	11.9±4.5
16	Ph	>361	—
17	CO_2Et	168±13.0	>5.8±0.0
18	$CONH_2$	>490	164.5±1.5
19	CO_2H	>408	>815
20	H	>248	>50
21	NHPh	>171	>34

[a]N = 2.
[b]CDC2/B $IC_{50} = 23.00 \pm 11.00\,\mu M$, cdk2/A $IC_{50} = 25.80 \pm 24.00\,\mu M$.

Table 2. Quinazoline substitution at the 4-position ($R^2 = CF_3$, $R^6 = H$)

Compounds	R^4	CDK4 IC_{50} (μM)	CDK2 IC_{50} (μM)
14	$NHC(CH_3)_3$	14.3±3.4	1.5±0.5
22	$NHC(CH_3)_2CH_2CH_3$	16.8±2.7	1.4±0.1
23	$NHSO_2CH(CH_3)_2$	>157	>31.0
24	$NHCH(CH_3)CH_2CH_2CH_3$	119.0±12.0	245.0±49.0
25	3-Hydroxypiperidine	>84	32.4±2.0
26	2-Hydroxymethylpyrolidine	63.0±0.0	14.8±0.2
27	$NHC(CH_3)_2CH_2OH$	15.0±0.0	2.3±0.5
28	$NHCH_2$(3′-F-Ph)	>39	15.6±1.2
29	$NHCH_2$(3′-F,5′-F-Ph)	>19	8.9±1.8
30	(*R*,*S*)-$NHCH(CH_3)$Ph	59	6.8
31	(*R*)-$NHCH(CH_3)$Ph	39.0±1.4	3.2±0.8
32	(*S*)-$NHCH(CH_3)$Ph	40[a]	31.0
33	(*R*,*S*)-$NHCH(CH_3)$(4′-F-Ph)	35[a]	16.5±3.5
34	$NHC(CH_3)_2$Ph	>151.0	14.0±1.4

[a]% activity at 50 μM.

for R^6 trifluoromethyl (**37**) and R^6 heteroaryl (**38**–**41**). Compound **37** was also notable for its approximately 50-fold selectivity for CDK2/E over CDK4/D and CDK6/D while maintaining a modest 2-fold selectivity with respect to CDK2/A.

A number of R^6 substituted phenyl groups were examined to determine if additional interaction with the ATP binding pocket could be exploited (Table 4). The 3-amino substituted analogue (**51**) was optimal, increasing activity 9-fold as compared to **13** in the CDK2/E assay.

Table 3. Quinazoline substitution at the 6-position (R^4 = NH*t*-Bu)

Compounds	R^2	$R^{6,7,8}$	CDK4 IC_{50} (μM)	CDK2 IC_{50} (μM)
35	CF_3	OH	18.00±0.00	1.150±0.210
36	CF_3	NHCOH	14.00±0.000	0.925±0.0071
37[a]	CF_3	CF_3	>37.00	0.790±0.000
38	CF_3	(3-Thiophene)	3.550±0.210	0.545±0.150
39	CF_3	(2-Furyl)	>3.00	1.20±0.140
40	CF_3	(2-Thiophene)	6.40±0.990	1.180±0.550
41	CF_3	(3-Pyridyl)	8.30±0.00	1.20±0.140

[a]CDK1/B IC_{50} >0.74 μM, CDK6/D2 IC_{50} = 56.00±1.40 μM, CDK2/A IC_{50} = 2.05±0.21 μM.

Table 4. 6-Substituted phenyl quinazolines ($R^2 = CF_3$, R^4 = NH*t*-Bu)

Compounds	R^6	CDK4 IC_{50} (μM)	CDK2 IC_{50} (μM)
42	Ph	7.7±1.0	1.8±0.1
43	2-MeOPh	>2.7	1.0±0.1
44	4-MeOPh	>27.0	10.0±2.8
45	4-HOPh	11.0±0.0	0.7±0.1
46	3-MeOPh	>6.7	3.3±0.3
47	3-HOPh	12.0±2.8	1.0±0.1
48	3-PyridylPh	8.3±0.0	1.2±0.1
49	4-ClPh	>26.0	2.6±0.9
50	2,4-DichloroPh	>2.4	>12.0
51	3-NH_2Ph	>2.1	0.6±0.1
52	4-NH_2Ph	>1.1	1.1±0.1
53	3-$CONH_2$Ph	>2.5	1.3± 0.1

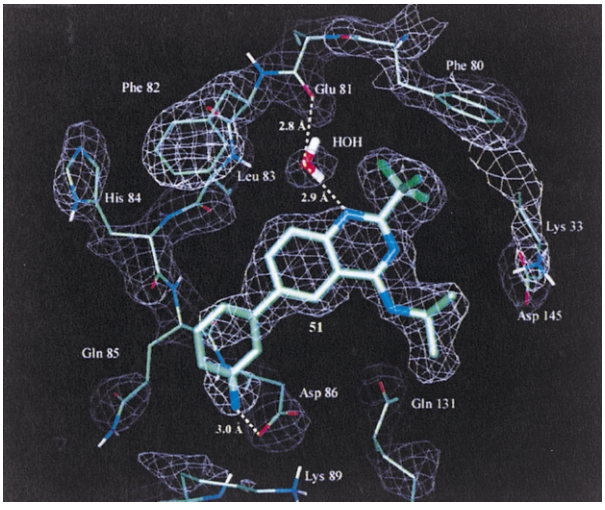

Figure 1. Crystal structure of CDK2 complexed with **51**.[9]

Compounds were evaluated for their ability to inhibit cell growth (Table 5). Quinazoline **36** showed the best translation into an HCT 116 cancer cell line, having low micromolar (IC_{50} = 5.72 μM) growth inhibition. Interestingly, normal human fibroblasts (AG1523)[7] tested under identical assay conditions were relatively insensitive to the inhibitors.

The crystal structure of human CDK2 complexed with **51** was determined to 2.0 Å resolution. The inhibitor binds into the ATP binding pocket located in the deep cleft between the upper and lower domains of CDK2.[8] Binding of **51** does not cause significant conformational changes in backbone atom positions as compared to the CDK2 apo enzyme structure[8] (0.72 Å rmsd). However, significant movements of side chains were observed for Lys33 (3.9 Å) and Lys89 (5.7 Å). These side-chain movements occurred to accommodate inhibitor binding. Residues within 3.5 Å of the inhibitor include Lys33, Phe80, Leu83, His84, Asp86, Lys89, and Asp145. The CDK2/**51** electron density maps suggest an indirect hydrogen bond between N1 and the backbone oxygen of Glu81 via a water molecule (Fig. 1). An additional hydrogen bond is observed between the side-chain oxygen of Asp86 and the N on R^6. There is a stacking interaction between the trifluoro group and Phe80. These interactions are unique to this series and represent an alternate binding mode to that reported for a series of 4-anilinoquinazolines.[13]

Employing solution-phase, parallel synthesis, a series of 4-aminosubstituted quinazoline CDK inhibitors was obtained. In interactions with CDK2/E complex, the 4-position of the quinazoline ring prefers small, branched alkyl groups and benzyl groups. This series of 4-aminoquinazolines has 5–20 times greater affinities for CDK2 as compared to CDK4 complexes. The 2-position of the quinazoline prefers the trifluoromethyl group while the 6-position is sensitive to both size and electronics as exemplified by **38** (CDK2/cyclin E IC_{50} = 0.54 μM) and **51** (CDK2/cyclin E IC_{50} = 0.65 μM). The effects on the cell cycle of representative compound **13** were consistent with CDK2/CDK4 inhibition. The crystal structure of **51** with CDK2 indicates that it binds in the ATP pocket of CDK2 and has an indirect hydrogen bond backbone oxygen of Glu81 via a water molecule. Overall, the quinazoline series represents a novel core in the inhibition of cyclic-dependent kinases with submicromolar potency.

Table 5. Quinazolines dosed in HCT116 cell assay

Compounds	SRB HCT 116 IC_{50} (μM)	SRB AG1523 IC_{50} (μM)
13	25.00±1.40	—
14	20.60±4.80	>74.00±0.00
35	7.30±0.64	>18.00
36	5.72±0.44	—
37	18.60±4.30	>59.00
38	18.40±1.10	>28.00±0.00

Acknowledgements

The authors would like to thank Marc Arnone, Melissa J. Ashbacher, Debra Doleniak, Laura Handel, Marv Kendal, Lynn Leffet, Diane Sharp, Fariba Shoarinejad, Lisa Sisk, Marge Stafford, and Ann Klemm for their efforts in carrying out the in vitro assays.

References and Notes

1. Pines, J. *Adv. Cancer Res.* **1995**, *66*, 181.
2. Sielecki, T. M.; Boylan, J. F.; Benfield, P. A.; Trainor, G. L. *J. Med. Chem.* **2000**, *43*, 1.
3. Senderowicz, A. M.; Headlee, D.; Stinson, S. F.; Lush, R. M.; Kalil, N.; Villalba, L.; Hill, K.; Steinberg, S. M.; Figg, W. D.; Tompkins, A.; Arbuck, S. G.; Sausville, E. A. *J. Clin. Oncol.* **1998**, *16*, 2986.
4. Zaharevitz, D.; Kunick, C.; Schultz, C.; Meijer, L.; Leost, M.; Gussio, R.; Senderowicz, A.; Lahusen, T.; Sausville, E. *Amer. Assoc. Cancer Res.*, April 10–14, 1999, Philadelphia, PA.
5. (a) Vesely, J.; Havlicek, L.; Strnad, M.; Blow, J. J.; Donella-Deana, A.; Pinna, L.; Letham, D. S.; Kato, J. Y.; Detivaud, L.; Leclerc, S.; Meijer, L. *Eur. J. Biochem.* **1994**, *224*, 771. (b) Abraham, R. T.; Acquarone, M.; Andersen, A.; Asensi, A.; Belle, R.; Berger, F.; Bergounioux, C.; Brunn, G.; Buquet-Fagot, C.; Fagot, D.; Glab, N.; Goudeau, M.; Guerrier, P.; Houghton, P. J.; Hendriks, H.; Kloareg, B.; Lippai, M.; Marie, D.; Maro, B.; Meijer, L.; Mester, J.; Mulner-Lorillon, O.; Poulet, S. A.; Schierenberg, E.; Schutte, B.; Vaulot, D.; Verlhac, M. H. *Biol. Cell* **1995**, *83*, 105. (c) Schutte, B.; Nieland, L.; van Engeland, M.; Henfling, M.; Meijer, L.; Ramaekers, F. *Exp. Cell. Res.* **1997**, *236*, 4.
6. (a) Singh, P.; Kumar, R. *J. Enzyme Inhib.* **1998**, *13*, 125. (b) Gibson, K. H.; Brundy, W.; Godfrey, A. A.; Woodburn, J. R.; Ashton, S. E.; Curry, B. J.; Scarlett, L.; Barker, A. J.; Brown, D. S. *Bioorg. Med. Chem. Lett.* **1997**, *7*, 2723. (c) Thompson, A. M.; Murray, D. K.; Elliott, W. L.; Fry, D. W.; Nelson, J. A.; Showalter, H. D.; Roberts, B. J.; Vincent, P. W.; Denny, W. A. *J. Med. Chem.* **1997**, *40*, 3915. (d) Myers, M. R.; Setzer, N. N.; Spada, A. P.; Persons, P. E.; Ly, C. Q.; Maguire, M. P.; Zulli, A. L.; Cheney, D. L.; Zilberstein, A.; Johnson, S. E.; Franks, C. F.; Mitchell, K. J. *Bioorg. Med. Chem. Lett.* **1997**, *7*, 421. (e) Myers, M. R.; Setzer, N. N.; Spada, A. P.; Zulli, A. L.; Hsu, C. J.; Zilberstein, A.; Johnson, S. E.; Hook, L. E.; Jacoski, M. V. *Bioorg. Med. Chem. Lett.* **1997**, *7*, 417.
7. Human foreskin fibroblasts (line AG01523) were purchased from the N.I.A. Aging Cell Culture Repository, Coriell Institute for Medical Research (Camden, NJ). Cells were routinely grown in Eagle's MEM containing 20% FBS and a 2× concentration of essential and non-essential amino acids and vitamins. Cultures were weaned onto 10% FBS over a two week period before experiments.
8. (a) DeBondt, H. L.; Rosenblatt, J.; Jancarik, J.; Jones, H. D.; Morgan, D. O.; Kim, S.-H. *Nature* **1993**, *363*, 595. (b) Schulze-Gahmen, U.; DeBondt, H. L.; Kim, S.-H. *J. Med. Chem.* **1996**, *39*, 4540.
9. Protein purification, crystallization, and structure determination: CDK2 protein was prepared and purified as described[10] with slight modifications including the addition of 10% (v/v) glycerol during the SP-sepharose and ATP-agarose column steps. CDK2 protein was concentrated to 6 mg/mL using a Collodion concentrator against 10 mM HEPES pH 7.4, 15 mM NaCl. Crystals were grown by vapor diffusion at 18 °C from sitting drops containing premixed and filtered (0.22 μm) solutions of 3.0 mg/mL CDK2, 32.5 mM HEPES (pH 7.4), 11.3 mM NaCl, 12.5 mM ammonium acetate, 2 mM DTT, 2–4% PEG 4000 against 100 mM HEPES (pH 7.4), 50 mM ammonium acetate, 2 mM DTT, 4–14% PEG 4000. CDK2 crystals were transferred to a solution containing 10 mM HEPES (pH 7.4), 15 mM NaCl, 1.0 mM **51**, 5.0% DMSO and soaked with inhibitor for 4 days. Crystals of CDK2/**51** were briefly transferred into cryo-protectant (10 mM HEPES pH 7.4, 15 mM NaCl, 25% MPD) and flash frozen in liquid nitrogen in preparation for cryo-data collection. Diffraction data were collected at −170 °C at the DND-CAT beam line, Advanced Photon Source, Argonne National Laboratories. Data were processed and scaled with HKL.[11] Crystals were orthorhombic and belonged to the space group $P2_12_12_1$ with unit cell dimensions $a = 71.96$ Å, $b = 73.51$ Å, $c = 54.28$ Å, $\alpha = \beta = \gamma = 90.0°$. Data is 98% complete to 2.0 Å resolution with an overall R-merge of 8.0%. Initial rigid body refinements[12] of the apo CDK2[8a] structure against the CDK2/**51** data were unsuccessful (R-factor = 47.0%). A translation search[12] found the highest peak in fractional coordinates at $x = 0.47$, $y = 0.019$, $z = 0.000$. Subsequent rigid body refinements lowered the R-factor to 33.2%. The Fo-Fc electron density map revealed the position of inhibitor in the ATP binding pocket along with a water molecule sandwiched between the inhibitor and backbone oxygen of Glu81. The CDK2 + **51** + HOH structure (Fig. 1) was refined with XPLOR[12] to a final R-factor of 21.9% and an R-free of 27.4%.
10. Rosenblatt, J.; DeBondt, H.; Jancarik, J.; Morgan, D. O.; Kim, S.-H. *J. Mol. Biol.* **1993**, *230*, 1317.
11. Otwinowski, Z.; Minor, W. In *Methods in Enzymology Macromolecular Crystallography, part A*; Carter, C. W., Jr., Sweet, R. M., Eds.; Academic: New York, 1997; Vol. 276, pp 307–326.
12. Brünger, A. T.; Kuriyan, J.; Karplus, M. *Science* **1987**, *234*, 458.
13. Shewchuk, L.; Hassell, A.; Wisely, B.; Rocque, W.; Holmes, W.; Veal, J.; Kuyper, L. F. *J. Med. Chem.* **2000**, *43*, 133.